

Fast hybrid tempered ensemble transform filter formulation for Bayesian elliptical problems via Sinkhorn approximation

Sangeetika Ruchi¹, Svetlana Dubinkina¹, and Jana de Wiljes²

¹Centrum Wiskunde & Informatica, P.O. Box 94079, 1098 XG Amsterdam, The Netherlands

²University of Potsdam, Karl-Liebknecht-Str. 24/25, D-14476, Potsdam, Germany

Correspondence: Jana de Wiljes (wiljes@uni-potsdam.de)

Abstract. Identification of unknown parameters on the basis of partial and noisy data is a challenging task in particular in high-dimensional and nonlinear settings. Gaussian approximations to the problem, such as ensemble Kalman filtering, tend to be robust, computationally cheap and often produce astonishingly accurate estimations despite the simplifying underlying assumptions. Yet there is a lot of room for improvement specifically regarding a correct approximation of a non-Gaussian posterior distribution. The tempered ensemble transform particle filter is an adaptive sequential Monte Carlo method, where resampling is based on optimal transport mapping. Unlike ensemble Kalman filtering it does not require any assumptions regarding the posterior distribution and hence has shown to provide promising results for nonlinear non-Gaussian inverse problems. However, the improved accuracy comes with the price of much higher computational complexity and the method is not as robust as the ensemble Kalman filtering in high-dimensional problems. In this work, we add an entropy-inspired regularisation factor to the underlying optimal transport problem that allows to considerably reduce the high computational cost via Sinkhorn iterations. Further, the robustness of the method is increased via an ensemble Kalman filtering proposal step before each update of the samples, which is also referred to as hybrid approach. The promising performance of the introduced method is numerically verified by testing it on a steady-state single-phase Darcy flow model with two different permeability configurations. The results are compared to the output of ensemble Kalman filtering, and Markov Chain Monte Carlo methods results are computed as a benchmark.

1 Introduction

If a solution of a considered partial differential equations (PDE) is highly-sensitive to its parameters, accurate estimation of the parameters and their uncertainties is essential to obtain a correct approximation of the solution. Partial observations of the solution are then used to infer uncertain parameters by solving a PDE-constrained inverse problem. For instance one can approach such problems via methods induced by Bayes's formula (Stuart, 2010). More specifically the posterior probability density of the parameters given the data, is then computed on the basis of a prior probability density and a likelihood which is the conditional probability density associated with the given noisy observations. Well-posedness of an inverse problem and convergence to the true posterior in the limit of observational noise going to zero was proven for different priors and under assumptions on the parameter-to-observation map by Dashti and Stuart (2017), for example.

25 When aiming at practical applications as in oil reservoir management (Lorentzen et al., 2020) and meteorology (Houtekamer and Zhang, 2016) for example, the posterior is approximated by means of a finite set of samples. Markov chain Monte Carlo (MCMC) methods approximate the posterior with a chain of samples—a sequential update of samples according to the posterior. Typically, MCMC methods provide highly-correlated samples. Therefore, in order to sample the posterior correctly MCMC requires a long chain, especially in the case of a multi-modal or a peaked distribution. A peaked posterior is associated with
 30 very accurate observations. Therefore, unless a speed up is introduced in a MCMC chain (e.g., Cotter et al., 2013), MCMC is impractical for computationally expensive PDE models.

Adaptive Sequential Monte Carlo (SMC) methods are different approaches to approximate the posterior with an *ensemble* of samples by computing their probability (e.g, Vergé et al., 2015). Adaptive intermediate probability measures are introduced between the prior measure and the posterior measure to improve upon method divergence due to the curse of dimensionality fol-
 35 lowing Del Moral et al. (2006); Neal (2001). Moreover, sampling from an invariant Markov kernel with the target intermediate measure and the reference prior measure improves upon ensemble diversity due to parameters stationarity as shown by Beskos et al. (2015). However, when parameter space is high-dimensional, adaptive SMC requires computationally prohibitive ensemble sizes unless we approximate only the first two moments (e.g., Iglesias et al., 2018) or we sample highly-correlated samples (Ruchi et al., 2019).

40 Ensemble Kalman filtering (EnKF) approximates only the first two moments of the posterior, which makes it computationally attractive for estimating high-dimensional parameters. For linear problems, Blömker et al. (2019) showed well-posedness and convergence of EnKF for a fixed ensemble size and without any assumptions of Gaussianity. However for nonlinear problems, it has been shown by Oliver et al. (1996); Bardsley et al. (2014); Ernst et al. (2015); Liu et al. (2017) that an EnKF approximation is not consistent with the Bayesian approximation.

45 As a side remark, EnKF was originally proposed for estimating a dynamical state of a chaotic system (e.g., Burgers et al., 1998). It was latter shown by Anderson (2001) that EnKF can be used for parameter estimation by introducing a trivial dynamics to the unknown static parameter. We note that EnKF is well known under different names in different scientific communities. In the reservoir community it is Ensemble Randomized Maximum Likelihood (Chen and Oliver, 2012), multiple data assimilation (Emerick and Reynolds, 2013), and Randomize-Then-Optimize (Bardsley et al., 2014). In the numerical weather
 50 prediction community, it falls under a large umbrella of Ensemble of Data Assimilation, see Carrassi et al. (2018) for a recent review. In the inverse problem community, it is ensemble Kalman inversion (Chada et al., 2018).

In order to sample highly-correlated samples, one can employ optimal transport resampling that lies at the heart of the ensemble transform particle filter (ETPF) proposed by Reich (2013). An optimal transport map between two consecutive probability measures provides a direct sample-to-sample map with maximized sample correlation. Along the lines of an adaptive
 55 SMC approach a probability measure is described via the importance weights and the deterministic mapping replaces the traditional resampling step. A so-called tempered ensemble transform particle filter (TETPF) was proposed by Ruchi et al. (2019). Note that this ansatz does not require any distributional assumption for the posterior and it was shown by Ruchi et al. (2019) that TETPF provides encouraging results for nonlinear high-dimensional PDE-constrained inverse problems. However, the computational cost of solving an optimal transport problem in each iteration is considerably high.

60 In this work we address two issues arisen in the context of TETPF: (i) the immense computational costs of solving the associated optimal transport problem and (ii) the lack of robustness of the TETPF with respect to high-dimensional problems. More specifically, the performance of ETPF has been found to be highly-dependent on the initial guess. Although tempering restrains any sharp fail in the importance sampling step due to a poor initial ensemble selection, the number of required intermediate steps and the efficiency of ETPF still depends on the initialisation. The lack of robustness in high dimensions
65 can be addressed via a hybrid approach that combines a Gaussian approximation with a particle filter approximation (e.g., Santitissadeekorn and Jones, 2015). Different algorithms are created by Frei and Künsch (2013); Stordal et al. (2011), for example. In this paper, we adapt a hybrid approach of Chustagulprom et al. (2016) that uses EnKF as a proposal step for ETPF with a tuning parameter. Furthermore, it is well established that the computational complexity of solving an optimal transport problem can be significantly reduced via a Sinkhorn approximation by Cuturi (2013). This ansatz has been implemented
70 for the ETPF Acevedo et al. (2017).

Along the lines of Chustagulprom et al. (2016); de Wiljes et al. (2020), we propose a tempered ensemble transform particle filter with Sinkhorn approximation (TESPF) and a tempered hybrid approach.

The remainder of the manuscript is organised as follows: in Sect. 2, the inverse problem setting is presented. There we describe the tempered ensemble transform particle filter (TETPF) proposed by Ruchi et al. (2019). Furthermore, we introduce the
75 tempered ensemble transform particle filter with Sinkhorn approximation (TESPF), a tempered hybrid approach that combines EnKF and TETPF (hybrid EnKF-TETPF), and a tempered hybrid approach that combines EnKF and TESPf (hybrid EnKF-TESPf). We discuss computational complexities of all the presented techniques and provide corresponding pseudocodes in Appendix A. In Sect. 3, we apply the adaptive SMC methods to an inverse problem of inferring high-dimensional permeability parameters for a steady-state single-phase Darcy flow model. Permeability is parameterized following Ruchi et al. (2019),
80 where one configuration of parametrization leads to Gaussian posteriors, while another one to non-Gaussian posteriors. Finally, we draw conclusions in Sect. 4.

2 Bayesian inverse problem

We assume $\mathbf{u} \in \tilde{\mathcal{U}} \subset \mathbb{R}^n$ is a random variable that is related to partially observable quantities $\mathbf{y} \in \mathcal{Y} \subset \mathbb{R}^k$ by a nonlinear forward operator $G : \tilde{\mathcal{U}} \rightarrow \mathcal{Y}$, namely

$$85 \quad \mathbf{y} = G(\mathbf{u}).$$

Further $\mathbf{y}_{\text{obs}} \in \mathcal{Y}$ denotes a noisy observation of \mathbf{y} , i.e.,

$$\mathbf{y}_{\text{obs}} = \mathbf{y} + \boldsymbol{\eta}$$

where $\boldsymbol{\eta} \sim \mathcal{N}(\mathbf{0}, \mathbf{R})$ and $\mathcal{N}(\mathbf{0}, \mathbf{R})$ is a Gaussian distribution with zero mean and \mathbf{R} covariance matrix. The aim is to determine or approximate the posterior measure $\mu(\mathbf{u})$ conditioned on observations \mathbf{y}_{obs} and given a prior measure $\mu_0(\mathbf{u})$, which is referred

90 to as Bayesian inverse problem. The posterior measure is absolutely continuous with respect to the prior, i.e.,

$$\frac{d\mu}{d\mu_0}(\mathbf{u}) \propto g(\mathbf{u}; \mathbf{y}_{\text{obs}}), \quad (1)$$

where \propto is up to a constant of normalisation and g is referred to as the likelihood and depends on the forward operator G . The Gaussian observation noise of the observation \mathbf{y}_{obs} implies

$$g(\mathbf{u}; \mathbf{y}_{\text{obs}}) = \exp \left[-\frac{1}{2} (G(\mathbf{u}) - \mathbf{y}_{\text{obs}})' \mathbf{R}^{-1} (G(\mathbf{u}) - \mathbf{y}_{\text{obs}}) \right], \quad (2)$$

95 where $'$ denotes the transpose. In the following we will introduce a range of methods that can be employed to estimate solutions to the presented inverse problem under the overarching mantel of tempered Sequential Monte Carlo filters. Alongside these methods we will also proposed several important add-on tools required to achieve feasibility and higher accuracy in high-dimensional nonlinear settings.

2.1 Tempered Sequential Monte Carlo

100 We consider sequential Monte Carlo (SMC) methods that approximate the posterior measure $\mu(\mathbf{u})$ via an empirical measure

$$\mu^M(\mathbf{u}) = \sum_{i=1}^M w_i \delta_{\mathbf{u}_i}(\mathbf{u}).$$

Here δ is the Dirac function, and the importance weights for the approximation of μ are

$$w_i = \frac{g(\mathbf{u}_i; \mathbf{y}_{\text{obs}})}{\sum_{j=1}^M g(\mathbf{u}_j; \mathbf{y}_{\text{obs}})}.$$

An ensemble $\mathcal{U} = \{\mathbf{u}_1, \dots, \mathbf{u}_M\} \subset \tilde{\mathcal{U}}$ consists of M realizations $\mathbf{u}_i \in \mathbb{R}^n$ of a random variable \mathbf{u} that are independent and
105 identically distributed according to $\mathbf{u}_i \sim \mu_0$.

When an easy-to-sample from prior μ_0 does not approximate the complex posterior μ well, only a few weights w_i have significant value resulting in a degenerative approximation of the posterior measure. Potential reasons for this effect are high dimensionality of the uncertain parameter, large number of observations, or accuracy of the observations. An existing solution to a degenerative approximation is an iterative approach based on tempering by Del Moral et al. (2006) or annealing by Neal
110 (2001). The underlying idea is to introduce T intermediate artificial measures $\{\mu_t\}_{t=0}^T$ between μ_0 and $\mu_T = \mu$. These measures are bridged by introducing T tempering parameters $\{\phi_t\}_{t=1}^T$ that satisfy $0 = \phi_0 < \phi_1 < \dots < \phi_T = 1$. An intermediate measure μ_t is defined as a probability measure that has density proportional to $g(\mathbf{u})$ with respect to the previous measure μ_{t-1}

$$\frac{d\mu_t}{d\mu_{t-1}}(\mathbf{u}) \propto g(\mathbf{u}; \mathbf{y}_{\text{obs}})^{(\phi_t - \phi_{t-1})}.$$

Along the lines of Iglesias (2016) the tempering parameter ϕ_t is chosen such that effective ensemble size (ESS)

$$115 \quad \text{ESS}_t(\phi) = \frac{\left(\sum_{i=1}^M w_{t,i} \right)^2}{\sum_{i=1}^M w_{t,i}^2}$$

with

$$w_{t,i} = \frac{g(\mathbf{u}_{t-1,i}; \mathbf{y}_{\text{obs}})^{(\phi_t - \phi_{t-1})}}{\sum_{j=1}^M g(\mathbf{u}_{t-1,j}; \mathbf{y}_{\text{obs}})^{(\phi_t - \phi_{t-1})}}, \quad (3)$$

does not drop below a certain threshold $1 < M_{\text{thresh}} < M$. Then an approximation of the posterior measure μ_t is

$$\mu_t^M(\mathbf{u}) = \sum_{i=1}^M w_{t,i} \delta_{\mathbf{u}_{t-1,i}}(\mathbf{u}). \quad (4)$$

120 A bisection algorithm on the interval $(\phi_{t-1}, 1]$ is employed to find ϕ . If $\text{ESS}_t > M_{\text{thresh}}$ we set $\phi_t = 1$ which implies that no further tempering is required.

The choice of ESS to define a tempering parameter is supported by results of Beskos et al. (2014) on stability of a tempered SMC method in terms of ESS. Moreover, for a Gaussian probability density approximated by importance sampling, Agapiou et al. (2017) showed that ESS is related to the second moment of the Radon-Nikodym derivative Eq. (1).

125 SMC method with importance sampling Eq. (4) does not change the sample $\{\mathbf{u}_{t-1,i}\}_{i=1}^M$, which leads to the method collapse due to a finite ensemble size. Therefore each tempering iteration t needs to be supplied with resampling. Resampling provides a new ensemble $\{\tilde{\mathbf{u}}_{t,i}\}_{i=1}^M$ that approximates the measure μ_t . We will discuss different resampling techniques in Sect. 2.3.

2.2 Mutation

Due to stationarity of the parameters SMC methods require ensemble perturbation. In the framework of particle filtering for
130 dynamical systems, ensemble perturbation is achieved by rejuvenation, when ensemble members of the posterior measure are perturbed with a random noise sampled from a Gaussian distribution with zero mean and a covariance matrix of the prior measure. The covariance matrix of the ensemble is inflated and no acceptance step is performed due to the associated high computational costs for a dynamical system.

Since we consider a static inverse problem, for ensemble perturbation we employ a Metropolis–Hastings method (thus we
135 mutate samples) but with a proposal that speeds up MCMC method for estimating a high-dimensional parameter. Namely, we use ensemble mutation of Cotter et al. (2013) with the target measure μ_t and the reference measure μ_0 . The mutation phase is initialized at $\mathbf{v}_{0,i} = \tilde{\mathbf{u}}_{t,i}$, and at the final inner iteration τ_{max} we assign $\mathbf{u}_{t,i} = \mathbf{v}_{\tau_{\text{max}},i}$ for $i = 1, \dots, M$.

For a Gaussian prior we use the preconditioned Crank-Nicolson MCMC (pcn-MCMC) method

$$\mathbf{v}_i^{\text{prop}} = \sqrt{1 - \theta^2} \mathbf{v}_{\tau,i} + (1 - \sqrt{1 - \theta^2}) \mathbf{m} + \theta \boldsymbol{\xi}_{\tau,i} \quad \text{for } i = 1, \dots, M. \quad (5)$$

140 Here \mathbf{m} is the mean of the Gaussian prior measure μ_0 and $\{\boldsymbol{\xi}_{\tau,i}\}_{i=1}^M$ are from a Gaussian distribution with zero mean and a covariance matrix of the Gaussian prior measure μ_0 .

For a uniform prior $U[a, b]$ we use the following random walk

$$\mathbf{v}_i^{\text{prop}} = \mathbf{v}_{\tau,i} + \boldsymbol{\xi}_{\tau,i} \quad i = 1, \dots, M. \quad (6)$$

Here $\{\xi_{\tau,i}\}_{i=1}^M \sim U[a-b, b-a]$ and $\{\mathbf{v}_i^{\text{prop}}\}_{i=1}^M$ are projected onto the $[a, b]$ interval if necessary. Then the ensemble at the
145 inner iteration $\tau + 1$ is

$$\mathbf{v}_{\tau+1,i} = \mathbf{v}_i^{\text{prop}} \quad \text{with the probability} \quad \rho(\mathbf{v}_i^{\text{prop}}, \mathbf{u}_{t-1,i}) \quad \text{for} \quad i = 1, \dots, M; \quad (7)$$

$$\mathbf{v}_{\tau+1,i} = \mathbf{v}_{\tau,i} \quad \text{with the probability} \quad 1 - \rho(\mathbf{v}_i^{\text{prop}}, \mathbf{u}_{t-1,i}) \quad \text{for} \quad i = 1, \dots, M. \quad (8)$$

Here $\mathbf{v}_i^{\text{prop}}$ is from Eq. (5) for the Gaussian measure and from Eq. (6) for the uniform measure, and

$$\rho(\mathbf{v}_i^{\text{prop}}, \mathbf{u}_{t-1,i}) = \min \left\{ 1, \frac{g(\mathbf{v}_i^{\text{prop}}; \mathbf{y}_{\text{obs}})^{\phi_t}}{g(\mathbf{u}_{t-1,i}; \mathbf{y}_{\text{obs}})^{\phi_t}} \right\}.$$

150 The scalar $\theta \in (0, 1]$ in Eq. (5) controls the performance of the Markov chain. Small values of θ lead to high acceptance rates but poor mixing. Roberts and Rosenthal (2001) showed that for high-dimensional problems it is optimal to choose θ such that the acceptance rate is in between 20 % and 30 % by the last tempering iteration T . Cotter et al. (2013) proved that under some assumptions this mutation produces a Markov kernel with an invariant measure μ_t .

Computational complexity. In each tempering iteration t the computational complexity of the pcn-MCMC mutation is
155 $\mathcal{O}(\tau_{\max} MC)$, where \mathcal{C} is the computational cost of the forward model G . For the pseudocode of the pcn-MCMC mutation please refer to the Algorithm 1 in Appendix A. Note that the computational complexity is not affected by the length of \mathbf{u} which is a very desirable property in high dimensions as shown by Cotter et al. (2013) and Hairer et al. (2014).

2.3 Resampling phase

As we have already mentioned in Sect. 2.1, an adaptive SMC method with importance sampling needs to be supplied with
160 resampling at each tempering iteration t . We consider a resampling method based on optimal transport mapping proposed by Reich (2013).

2.3.1 Optimal transformation

The origin of the optimal transport theory lies in finding an optimal way of redistributing mass which was first formulated by Monge (1781). Given a distribution of matter, e.g., a pile of sand, the underlying question is how to reshape the matter into
165 another form such that the work done is minimal. A century later the original problem was rewritten by Kantorovich (1942) in a statistical framework that allowed to tackle it. Due to these contributions it was later named the Monge-Kantorovich minimization problem. The reader is also referred to Peyré and Cuturi (2019) for a comprehensible overview.

Let us consider a scenario where the initial distribution of matter is represented by a probability measure μ on the measurable space $\tilde{\mathcal{U}}$, that has to be moved and rearranged according to a given new distribution ν , defined on the measurable space $\tilde{\mathcal{V}}$. Then
170 we seek a probability measure that is a solution to

$$\inf \left\{ \int_{\tilde{\mathcal{U}} \times \tilde{\mathcal{V}}} c(\mathbf{u}, \tilde{\mathbf{u}}) d\omega : \quad \omega \in \Pi(\mu, \nu) \right\}, \quad (9)$$

where the minimum is computed over all joint probability measures ω on $\tilde{\mathcal{U}} \times \tilde{\mathcal{V}}$ with marginals μ and ν , and $c(\mathbf{u}, \tilde{\mathbf{u}})$ is a transport cost function on $\tilde{\mathcal{U}} \times \tilde{\mathcal{V}}$. The joint measures achieving the infimum are called optimal transport plans.

Let μ and ν be two measures on a measurable space (Ω, \mathcal{F}) such that μ is the law of random variable $U: \Omega \rightarrow \tilde{\mathcal{U}}$ and ν is the law of random variable $V: \Omega \rightarrow \tilde{\mathcal{V}}$. Then a coupling of (μ, ν) consists of a pair (U, V) . Note that couplings always exist, an example is the trivial coupling in which the random variables U and V are independent. A coupling is called deterministic if there exists a measurable function $\Psi_M: \tilde{\mathcal{U}} \rightarrow \tilde{\mathcal{V}}$ such that $V = \Psi_M(U)$ and Ψ_M is called transport map. Unlike general couplings, deterministic couplings do not always exist. On the other hand there may be infinitely many deterministic couplings. One famous variant of Eq. (9), where the optimal coupling is known to be a deterministic coupling, is given by

$$\omega^* = \arg \inf \left\{ \int_{\tilde{\mathcal{U}} \times \tilde{\mathcal{V}}} \|\mathbf{u} - \tilde{\mathbf{u}}\|^2 d\omega(\mathbf{u}, \tilde{\mathbf{u}}) : \omega \in \Pi(\mu, \nu) \right\}. \quad (10)$$

The aim of the resampling step is to obtain equally probable samples. Therefore, in resampling based on optimal transport of Reich (2013), the Monge-Kantorovich minimization problem Eq. (10) is considered for the current posterior measure $\mu_t^M(\mathbf{u})$ given by its samples approximation Eq. (4) and a uniform measure (here the weights in the sample approximation are set to $1/M$). The discretized objective functional of the associate optimal transport problem is given by

$$J(\mathbf{S}) := \sum_{i,j=1}^M s_{ij} \|\mathbf{u}_{t-1,i} - \mathbf{u}_{t-1,j}\|^2$$

subject to $s_{ij} > 0$ and constraints

$$\sum_{i=1}^M s_{ij} = \frac{1}{M}, \quad j = 1, \dots, M; \quad \sum_{j=1}^M s_{ij} = w_{t,i}, \quad i = 1, \dots, M,$$

where matrix \mathbf{S} describes a joint probability measure under the assumption that the state space is finite. Then samples $\{\tilde{\mathbf{u}}_{t,i}\}_{i=1}^M$ are obtained by a deterministic linear transform, i.e.,

$$\tilde{\mathbf{u}}_{t,j} := M \sum_{i=1}^M \mathbf{u}_{t-1,i} s_{ij} \quad \text{for } j = 1, \dots, M. \quad (11)$$

Reich (2013) showed weak convergence of the deterministic optimal transformation Eq. (11) to a solution of the Monge-Kantorovich problem Eq. (9) as $M \rightarrow \infty$.

Computational complexity. The computational complexity of solving the optimal transport problem with an efficient earth mover distance algorithm such as FastEMD of Pele and Werman (2009) is of order $\mathcal{O}(M^3 \log M)$. Consequently the computational complexity of the adaptive tempering SMC with optimal transport resampling (TETPF) is $\mathcal{O}[T(MC + M^3 \log M + \tau_{\max} MC)]$, where T is the number of tempering iterations, τ_{\max} is the number of pcn-MCMC inner iterations, and \mathcal{C} is computational cost of a forward model G . For the pseudocode of the TETPF please refer to the Algorithm 4 in Appendix A.

2.3.2 Sinkhorn approximation

As discussed above solving the optimal transport problem has a computational complexity of $\mathcal{O} = M^3 \log(M)$ in every iteration of the tempering procedure. Thus the TETPF becomes very expensive for large M . On the other hand an increase in the number of samples directly correlates with an improved accuracy of the estimation. In order to allow for as many samples as possible one needs to reduce the associated computational cost of the optimal transport problem. This can be achieved by replacing the optimal transport distance with a Sinkhorn distance and subsequently exploiting the new structure to elude the immense computational time of the EMD solver as shown by Cuturi (2013). More precisely the ansatz is built on the fact that the original transport problem has a natural entropic bound that is obtained for $\mathbf{S} = [\frac{1}{M} \mathbf{I}_M \mathbf{w}^\top]$ where $\mathbf{w} = [w_1, \dots, w_M]$ and $\mathbf{I}_M = [1, \dots, 1] \in \mathbb{R}^M$ which constitutes an independent joint probability. Therefore, one can consider the problem of finding a matrix $\mathbf{S} \in \mathbb{R}^{M \times M}$ that is constrained by an additional lower entropic bound (Sinkhorn distance). This additional constraint can be incorporated via a Lagrange multiplier, which leads to the above regularised form, i.e.,

$$J_{\text{SH}}(\mathbf{S}) = \sum_{i,j=1}^M \left\{ s_{ij} \|\mathbf{u}_{t-1,i} - \mathbf{u}_{t-1,j}\|^2 + \frac{1}{\alpha} s_{ij} \log s_{ij} \right\} \quad (12)$$

where $\alpha > 0$. Due to additional smoothness the minimum of Eq. (12) can be unique and has the form

$$\mathbf{S}^\alpha = \mathbf{diag}(\mathbf{b}) \exp(-\alpha \mathbf{Z}) \mathbf{diag}(\mathbf{a})$$

where \mathbf{Z} is matrix with entries $z_{ij} = \|\mathbf{u}_{t-1,i} - \mathbf{u}_{t-1,j}\|^2$ and \mathbf{b} and \mathbf{a} non-negative vectors determined by employing Sinkhorn's fixpoint iteration described by Sinkhorn (1967). We will refer to this approach as tempered ensemble Sinkhorn particle filter (TESPF).

Computational complexity. Solving this regularised optimal transport problems rather than original transport problem given in Eq. (9) reduces the complexity to $\mathcal{O}(M^2 C(\alpha))$. Note however that $C(\alpha)$ depends on the chosen regularisation and grows with α . Therefore, one needs to balance between reducing computational time and finding a reasonable approximate solution of the original transport problem when choosing a value for α . For the pseudocode of the Sinkhorn adaptation of solving the optimal transport problem please refer to the Algorithm 3 in Appendix A. For the pseudocode of the TESPf please refer to the Algorithm 4 in Appendix A.

2.4 Ensemble Kalman Filter

For Bayesian inverse problems with Gaussian measures, ensemble Kalman filter (EnKF) is one of the widely used algorithms. EnKF is an adaptive SMC method that approximates the first two statistical moments of a posterior distribution. For a linear forward model, EnKF is optimal in a sense it minimizes the error in the mean (Blömker et al., 2019). For a nonlinear forward model, EnKF still provides a good estimation of the posterior (e.g., Iglesias et al., 2018). Here we consider EnKF method of Iglesias et al. (2018), since it is based on the tempering approach.

The intermediate measures $\{\mu_t\}_{t=0}^T$ are approximated by Gaussian distributed variables with empirical mean \mathbf{m}_t and empirical variance \mathbf{C}_t . Empirical mean \mathbf{m}_{t-1} and empirical covariance \mathbf{C}_{t-1} are defined in terms of $\{\mathbf{u}_{t-1,i}\}_{i=1}^M$ as following

$$\mathbf{m}_{t-1} = \frac{1}{M} \sum_{i=1}^M \mathbf{u}_{t-1,i}, \quad \mathbf{C}_{t-1} = \frac{1}{M-1} \sum_{i=1}^M (\mathbf{u}_{t-1,i} - \mathbf{m}_{t-1}) \otimes (\mathbf{u}_{t-1,i} - \mathbf{m}_{t-1}),$$

230 where \otimes denotes Kroneker product. Then the mean and the covariance are updated as

$$\mathbf{m}_t = \mathbf{m}_{t-1} + \mathbf{C}_{t-1}^{\text{uG}} (\mathbf{C}_{t-1}^{\text{GG}} + \Delta_t \mathbf{R})^{-1} (\mathbf{y}_{\text{obs}} - \bar{\mathbf{G}}_{t-1}) \quad \text{and} \quad \mathbf{C}_t = \mathbf{C}_{t-1} - \mathbf{C}_{t-1}^{\text{uG}} (\mathbf{C}_{t-1}^{\text{GG}} + \Delta_t \mathbf{R})^{-1} (\mathbf{C}_{t-1}^{\text{uG}})',$$

respectively. Here $'$ denotes the transpose,

$$\mathbf{C}_{t-1}^{\text{uG}} = \frac{1}{M-1} \sum_{i=1}^M (\mathbf{u}_{t-1,i} - \mathbf{m}_{t-1}) \otimes (G(\mathbf{u}_{t-1,i}) - \bar{\mathbf{G}}_{t-1}), \quad \mathbf{C}_{t-1}^{\text{GG}} = \frac{1}{M-1} \sum_{i=1}^M [G(\mathbf{u}_{t-1,i}) - \bar{\mathbf{G}}_{t-1}] \otimes [G(\mathbf{u}_{t-1,i}) - \bar{\mathbf{G}}_{t-1}],$$

$$235 \quad \bar{\mathbf{G}}_{t-1} = \frac{1}{M} \sum_{i=1}^M G(\mathbf{u}_{t-1,i}), \quad \text{and} \quad \Delta_t = \frac{1}{\phi_t - \phi_{t-1}}.$$

We recall that the nonlinear forward problem is $\mathbf{y} = G(\mathbf{u})$, the observation \mathbf{y}_{obs} has a Gaussian observation noise with zero mean and the covariance matrix \mathbf{R} , and ϕ_t is a temperature associated with the measure μ_t .

Since we are interested in an ensemble approximation of the posterior distribution, we update the ensemble members by

$$\tilde{\mathbf{u}}_{t,i} = \mathbf{u}_{t-1,i} + \mathbf{C}_{t-1}^{\text{uG}} (\mathbf{C}_{t-1}^{\text{GG}} + \Delta_t \mathbf{R})^{-1} [\mathbf{y}_{t,i} - G(\mathbf{u}_{t-1,i})] \quad \text{for } i = 1, \dots, M. \quad (13)$$

240 Here $\mathbf{y}_{t,i} = \mathbf{y}_{\text{obs}} + \boldsymbol{\eta}_{t,i}$ and $\boldsymbol{\eta}_{t,i} \sim \mathcal{N}(\mathbf{0}, \Delta_t \mathbf{R})$ for $i = 1, \dots, M$.

Computational complexity. The computational complexity of solving Eq. (13) is $\mathcal{O}(\kappa^2 n)$, where n is the parameter space dimension, and κ is the observation space dimension. Then the computational complexity of EnKF is $\mathcal{O}[T(MC + \kappa^2 n + \tau_{\text{max}} MC)]$, where T is the number of tempering iterations, τ_{max} is the number of pcn-MCMC inner iterations, and \mathcal{C} is computational cost of a forward model G . For the pseudocode of the EnKF method please refer to the Algorithm 5 in Appendix A.

245 2.5 Hybrid

Despite the underlying Gaussian assumption the EnKF is remarkably robust in nonlinear high-dimensional settings opposed to consistent SMC methods such as the TET(S)PF. For many nonlinear problems it is desirable to have better uncertainty estimates while maintaining a level of robustness. This can be achieved by factorising the likelihood given by Eq. (2), e.g,

$$g(\mathbf{u}; \mathbf{y}_{\text{obs}}) = g_1(\mathbf{u}; \mathbf{y}_{\text{obs}}) \cdot g_2(\mathbf{u}; \mathbf{y}_{\text{obs}}),$$

250 where

$$g_1(\mathbf{u}; \mathbf{y}_{\text{obs}}) = g(\mathbf{u}; \mathbf{y}_{\text{obs}})^\beta = \exp \left[-\frac{1}{2} (G(\mathbf{u}) - \mathbf{y}_{\text{obs}})' (\beta \mathbf{R})^{-1} (G(\mathbf{u}) - \mathbf{y}_{\text{obs}}) \right] \quad (14)$$

and

$$g_2(\mathbf{u}; \mathbf{y}_{\text{obs}}) = g(\mathbf{u}; \mathbf{y}_{\text{obs}})^{(1-\beta)} = \exp \left[-\frac{1}{2} (G(\mathbf{u}) - \mathbf{y}_{\text{obs}})' [(1-\beta) \mathbf{R}]^{-1} (G(\mathbf{u}) - \mathbf{y}_{\text{obs}}) \right]. \quad (15)$$

Then it is possible to alternate between methods with complementing properties such as the EnKF and the TET(S)PF updates
 255 e.g., likelihood

$$\exp \left[-\frac{\beta}{2} (G(\mathbf{u}) - \mathbf{y}_{\text{obs}})' \mathbf{R}^{-1} (G(\mathbf{u}) - \mathbf{y}_{\text{obs}}) \right]^{(\phi_t - \phi_{t-1})}$$

is used for an EnKF update followed by an update with a TET(S)PF on the basis of

$$\exp \left[-\frac{(1-\beta)}{2} (G(\mathbf{u}) - \mathbf{y}_{\text{obs}})' \mathbf{R}^{-1} (G(\mathbf{u}) - \mathbf{y}_{\text{obs}}) \right]^{(\phi_t - \phi_{t-1})}.$$

Note that $\beta \in [0, 1]$ and should be tuned according to underlying forward operator. This combination of an approximative
 260 Gaussian method and a consistent SMC method has been referred to as hybrid filters in the data assimilation literature¹ (Stordal
 et al., 2011; Frei and Künsch, 2013; Chustagulprom et al., 2016). This ansatz can also be understood as using the EnKF as a
 more elaborate proposal density for the importance sampling step within SMC (e.g., Oliver et al., 1996).

Computational complexity. The computational complexity of combining the two algorithms is $\mathcal{O}[T(MC + \kappa^2 n + MC +$
 $M^3 \log M + \tau_{\max} MC)]$ for the hybrid EnKF-TETPF and $\mathcal{O}[T(MC + \kappa^2 n + MC + M^2 C(\alpha) + \tau_{\max} MC)]$ for the hybrid EnKF-
 265 TESPF. For the pseudocode of the hybrid methods please refer to the Algorithm 6 in Appendix A.

3 Numerical experiments

We consider a steady-state single-phase Darcy flow model defined over an aquifer of two-dimensional physical domain $D =$
 $[0, 6] \times [0, 6]$, which is given by

$$-\nabla \cdot [k(x, y) \nabla P(x, y)] = f(x, y), \quad (x, y) \in D, \quad (16)$$

270 where $\nabla = (\partial/\partial x \ \partial/\partial y)'$, \cdot the dot product, $P(x, y)$ the pressure, $k(x, y)$ the permeability, $f(x, y)$ the source term which
 accounts for groundwater recharge, and (x, y) are horizontal dimensions. The boundary conditions are

$$P(x, 0) = 100, \quad \frac{\partial P}{\partial x}(6, y) = 0, \quad -k(0, y) \frac{\partial P}{\partial x}(0, y) = 500, \quad \frac{\partial P}{\partial y}(x, 6) = 0, \quad (17)$$

where ∂D is the boundary of domain D . The source term is

$$f(x, y) = \begin{cases} 0 & \text{if } 0 < y \leq 4, \\ 137 & \text{if } 4 < y < 5, \\ 274 & \text{if } 5 < y \leq 6. \end{cases}$$

275 We implement a cell-centered finite-difference method and a linear algebra solver (backslash operator in MATLAB) to solve
 the forward model Eqs. (16)–(17) on an $N \times N$ grid.

¹Note that the terminology is also used in the context of data assimilation filters combining variational and sequential approaches.

(1986)

$$c(x, y) = \frac{1}{\gamma(1)} \frac{\|x - y\|}{v} \Upsilon_1 \left(\frac{\|x - y\|}{v} \right),$$

295 where γ is the gamma function, $v = 0.5$ is the characteristic length scale, and Υ_1 is the modified Bessel function of the second kind of order 1.

We denote by λ and \mathbf{V} eigenvalues and eigenfunctions of the corresponding covariance matrix \mathbf{C} , respectively. Then, following a Karhunen-Loeve expansion, log permeability is

$$\log(k^l) = \log(m) + \sum_{\ell=1}^{N^2} \sqrt{\lambda^\ell} V^{\ell l} u^\ell \quad \text{for } l = 1, \dots, N^2,$$

300 where u^ℓ is i.i.d. from $\mathcal{N}(0, 1)$ for $\ell = 1, \dots, N^2$.

For F1, the prior for log permeability is a Gaussian distribution with mean 5. The grid dimension is $N = 70$, and thus the uncertain parameter $\mathbf{u} = \{u^\ell\}_{\ell=1}^{N^2}$ has dimension 4900.

For F2, we assume geometrical parameters $\mathbf{d} = \{d^i\}_{i=1}^5$ are drawn from uniform priors, namely $d^1 \sim U[0.3, 2.1]$, $d^2 \sim U[\pi/2, 6\pi]$, $d^3 \sim U[-\pi/2, \pi/2]$, $d^4 \sim U[0, 6]$, $d^5 \sim U[0.12, 4.2]$. Furthermore, we assume independence between geometric
 305 parameters and log permeability. The prior for log permeability is a Gaussian distribution with mean 15 outside the channel and with mean 100 inside the channel. The grid dimension is $N = 50$. Log permeability inside channel $\mathbf{u}^1 = \{u^{1,\ell}\}_{\ell=1}^{N^2}$ and log permeability outside channel $\mathbf{u}^2 = \{u^{2,\ell}\}_{\ell=1}^{N^2}$ are defined over the entire domain 50×50 . Therefore, for F2 inference the uncertain parameter $\mathbf{u} = \{\mathbf{d}, \mathbf{u}^1, \mathbf{u}^2\}$ has dimension 5005. Moreover, for F2 we use the Metropolis-within-Gibbs methodology following Iglesias et al. (2014) to separate geometrical parameters and log permeability parameters within the mutation step,
 310 since it allows to better exploit the structure of the prior.

3.2 Observations

Both the true permeability and an initial ensemble are drawn from the same prior distribution as the prior includes knowledge about geological properties. However, an initial guess is computed on a coarse grid and the true solution is computed on a fine grid that has twice the resolution of the coarse grid. The synthetic observations of pressure are obtained by

$$315 \quad \mathbf{y}_{\text{obs}} = \mathbf{L}(\mathbf{P}^{\text{true}}) + \boldsymbol{\eta}.$$

An element of $\mathbf{L}(\mathbf{P}^{\text{true}})$ is a linear functional of pressure, namely

$$L^j(\mathbf{P}^{\text{true}}) = \frac{1}{2\pi\sigma^2} \sum_{i=1}^{N_f} \exp\left(-\frac{\|\mathbf{X}^i - \mathbf{h}^j\|^2}{2\sigma^2}\right) (P^{\text{true}})^j \Delta x^2 \quad \text{for } j = 1, \dots, \kappa.$$

Here $\sigma = 0.01$, Δx^2 is the size of a grid cell $\mathbf{X}^i = (X^i, Y^i)$, N_f is resolution of a fine grid, \mathbf{h}^j is the location of the observation and κ is the number of observations. This form of the observation functional and the parameterization F1 and F2 guaranty
 320 the continuity of the forward map from the uncertain parameters to the observations and thus the existence of the posterior

distribution as shown by Iglesias et al. (2014). The observation noise $\boldsymbol{\eta}$ is drawn from a normal distribution with zero mean and known covariance matrix \mathbf{R} . We choose the observation noise to be 2 % of L2-norm of the true pressure. With such a small noise the likelihood is a peaked distribution. Therefore, a non-iterative data assimilation approach requires a computationally unfeasible number of ensemble members to sample the posterior.

325 To save computational costs, we choose ESS threshold $M_{\text{thresh}} = M/3$ for tempering, and the length of Markov chain $\tau_{\text{max}} = 20$ for mutation.

3.3 Metrics

We conduct numerical experiments with ensemble sizes $M = 100$ and $M = 500$, and 20 simulations with different initial ensemble realizations to check the robustness of results. We analyze the method's performance with respect to a pcn-MCMC
330 solution from here on referred to as reference. An MCMC solution was obtained by combining 50 independent chains each of length 10^6 , 10^5 burn-in period and 10^3 thinning. For log permeability, we compute RMSE of the mean

$$\text{RMSE} = \sqrt{(\bar{\mathbf{u}} - \bar{\mathbf{u}}^{\text{ref}})'(\bar{\mathbf{u}} - \bar{\mathbf{u}}^{\text{ref}})}, \quad \text{where} \quad \bar{\mathbf{u}} = \frac{1}{M} \sum_{i=1}^M \mathbf{u}_i, \quad (18)$$

and \mathbf{u}^{ref} is the reference solution.

For geometrical parameters \mathbf{d} , we compute the Kullback-Leibler divergence

$$335 \quad D_{\text{KL}}^i(p^{\text{ref}} \| p) = \sum_{j=1}^{M_b} p^{\text{ref}}(d_j^i) \log \frac{p^{\text{ref}}(d_j^i)}{p(d_j^i)}, \quad (19)$$

where $p^{\text{ref}}(d^i)$ is the reference posterior, $p(d^i)$ is approximated by the weights, and $M_b = M/10$ is a chosen number of bins.

3.4 Application to F1 inference

For F1, we perform numerical experiments using 36 uniformly distributed observations, which are displayed in circles in Fig. 3(a). We plot a box plot of RMSE given by Eq. (18) over 20 independent simulations in Fig. 2(a) using Sinkhorn approxi-
340 mation and in Fig. 2(b) using optimal transport. The x-axis is for the hybrid parameter β , whose value 0 corresponds to EnKF and 1 to an adaptive SMC method with either a Sinkhorn approximation (TESPF) or optimal transport (TETPF). Ensemble size $M = 100$ is shown in red and $M = 500$ in green. First, we observe that at a small ensemble size $M = 100$ and a large β (namely $\beta \geq 0.6$) TESPf outperforms TETPF as the RMSE error is lower. Since Sinkhorn approximation is a regularization of an optimal transport solution, TESPf provides a smoother solution than TETPF that can be seen in Fig. 3(c) and Fig. 3(f),
345 respectively, where we plot mean log permeability. Next, we see in Fig. 2 that the hybrid approach decreases RMSE compared to TET(S)PF: the smaller β the smaller median of RMSE. EnKF gives the smallest error due to the Gaussian parametrization of permeability. The advantage of the hybrid approach is most pronounced at a large ensemble size $M = 500$ and optimal transport resampling. Furthermore, we note a discrepancy between the $M = 100$ and the $M = 500$ experiments at $\beta = 0$, thus EnKF alone. This is related to the curse of dimensionality. It appears that the ensemble size $M = 100$ is too small to estimate

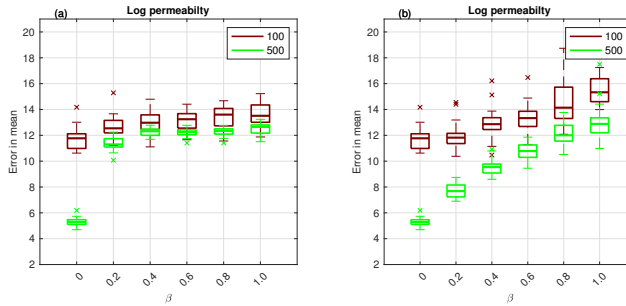


Figure 2. Application to F1 parameterization: using Sinkhorn approximation (a) and optimal transport resampling (b). Box plot over 20 independent simulations of RMSE of mean log permeability. X-axis is for the hybrid parameter, where $\beta = 0$ corresponds to EnKF and $\beta = 1$ to TET(S)PF. Ensemble size $M = 100$ is shown in red, and $M = 500$ in green. Central mark is the median, edges of the box are the 25th and 75th percentiles, whiskers extend to the most extreme datapoints, and crosses are outliers.

an uncertain parameter of the dimension 10^3 using 36 accurate observations. However, at the ensemble size $M = 500$ EnKF alone ($\beta = 0$) gives an excellent performance compared to any combination ($\beta > 0$).

We plot mean log permeability at ensemble size $M = 100$ and a smallest RMSE over 20 simulations in Fig. 3(b)–(f) and of reference in Fig. 3(a). We see that EnKF and TETPF(0.2) estimate well not only large-scale feature but also small-scale feature (e.g., negative mean at the top right corner) unlike TET(S)PF and TESPf(0.2).

3.5 Application to F2 inference

For F2, we perform numerical experiments using 9 uniformly distributed observations, which are displayed in circles in Fig. 9(a). First, we display results obtained by Sinkhorn approximation. In Fig. 4, we plot box plot over 20 independent runs of KL divergence given by Eq. (19) for amplitude (a), frequency (b), angle (c), initial point (d), and width (e) that define channel. We see that EnKF outperforms any TESPf(·) including TESPf for amplitude (a) and width (e). This is due to Gaussian-like posteriors of these two geometrical parameters displayed in Fig. 6(c) and Fig. 6(o), respectively. Due to Gaussian-like posteriors the hybrid approach decreases RMSE compared to TESPf: the smaller β the smaller median of RMSE.

For frequency, angle, and initial point, whose KL divergence is displayed in Fig. 4(b), (c), and (d), respectively, the behaviour of adaptive SMC is nonlinear in terms of β . This is due to non Gaussian-like posteriors of these three geometrical parameters shown in Fig. 6(f), (i), and (l), respectively. Due to non Gaussian-like posteriors the hybrid approach gives an advantage over both TESPf and EnKF—there exists a $\beta \neq 0$ for which the KL divergence is lowest although it is inconsistent between geometrical parameters.

When comparing TESPf(·) to TETPF(·), we observe the same type of behaviour in terms of β : linear for amplitude and width, whose KL divergence is displayed in Fig. 5(a) and (e), respectively, and nonlinear for frequency, angle, and initial point, whose KL divergence is displayed in Fig. 5(b), (c), and (d), respectively. However, the KL divergence is smaller when optimal transport resampling is used instead of Sinkhorn approximation.

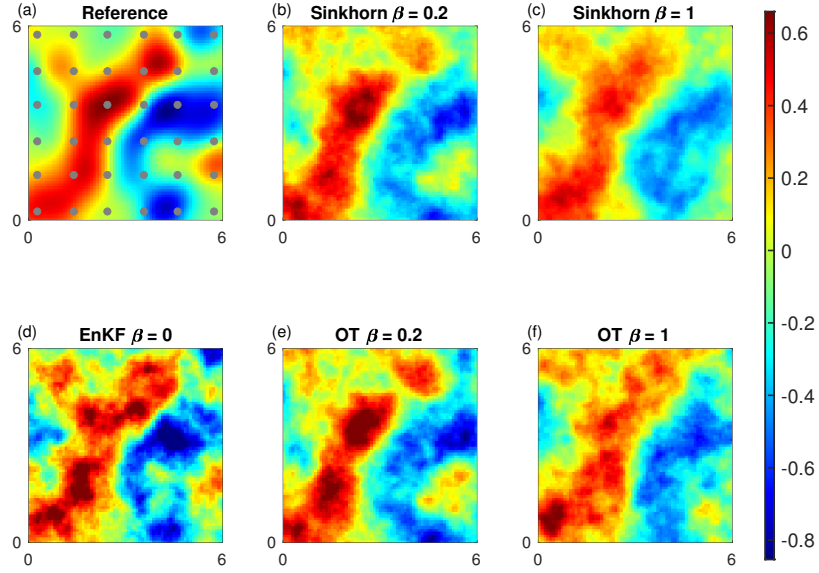


Figure 3. Mean log permeability for F1 inference for the lowest error at ensemble size $M = 100$. Observation locations are shown in circles. Reference (a), TESPf(0.2) (b), TESPf (c), EnKF (d), TETPF(0.2) (e), and TETPF (f).

In Fig. 6, we plot posterior of geometrical parameters: amplitude (a)–(c), frequency (d)–(f), angle (g)–(i), initial point (j)–(l), and width (m)–(o), where on the left TESPf(0.2), in the middle TETPF(0.2), and on the right EnKF are shown. In black is the reference, in red 20 simulations of ensemble size $M = 100$, in green 20 simulations of ensemble size $M = 500$. The true parameters are shown as black cross. We see that as ensemble size increases posteriors approximated by TET(S)PF converge to the reference posterior unlike EnKF.

Now we investigate adaptive SMC performance for permeability estimation. First, we display results obtained by Sinkhorn approximation. The box plot shows over 20 independent simulations of RMSE given by Eq. (18) for log permeability outside channel in Fig. 7(a) and inside channel in Fig. 7(b). Even though log permeability is Gaussian distributed, for a small ensemble size $M = 100$ there exists a $\beta \neq 0$ that gives lowest RMSE both outside and inside channel. As ensemble size increases, methods performance becomes equivalent.

Next, we compare TESPf(·) to TETPF(·) for log permeability estimation outside and inside channel whose RMSE is displayed in Fig. 8(a) and (b), respectively. We observe the same type of behaviour in terms of β : nonlinear for a small ensemble size $M = 100$, and equivalent for a larger ensemble size $M = 500$. Furthermore, at a small ensemble size $M = 100$ TESPf outperforms TETPF, which was also the case for F1 parameterization Sec. 3.4.

In Fig. 9, we show mean field of permeability over the channelized domain for reference for the lowest error at ensemble size $M = 100$ for TESPf(0.2) (b), TESPf (c), EnKF (d), TETPF(0.2) (e), and TETPF (f). We plot mean log permeability over

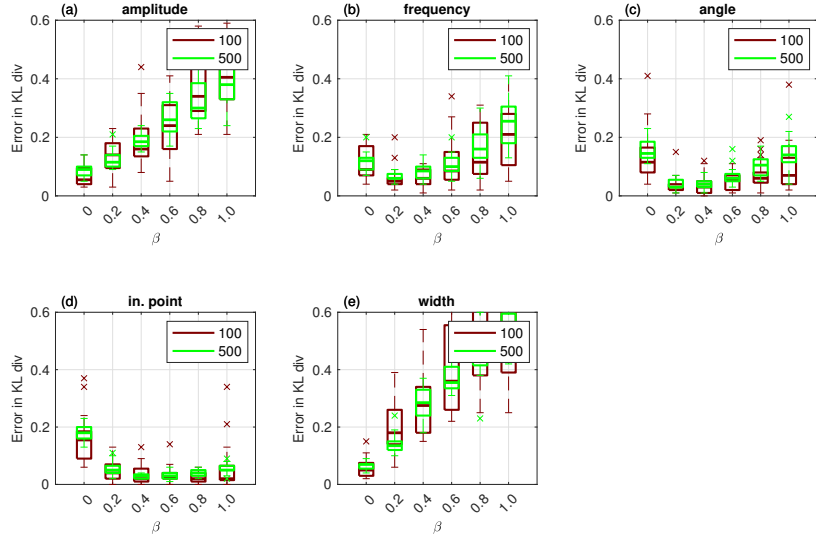


Figure 4. Application to F2 parameterization using Sinkhorn approximation. Box plot over 20 independent simulations of KL divergence for geometrical parameters: amplitude (a), frequency (b), angle (c), initial point (d), and width (e). X-axis is for the hybrid parameter, where $\beta = 0$ corresponds to EnKF and $\beta = 1$ to TET(S)PF. Ensemble size $M = 100$ is shown in red, and $M = 500$ in green. Central mark is the median, edges of the box are the 25th and 75th percentiles, whiskers extend to the most extreme datapoints, and crosses are outliers.

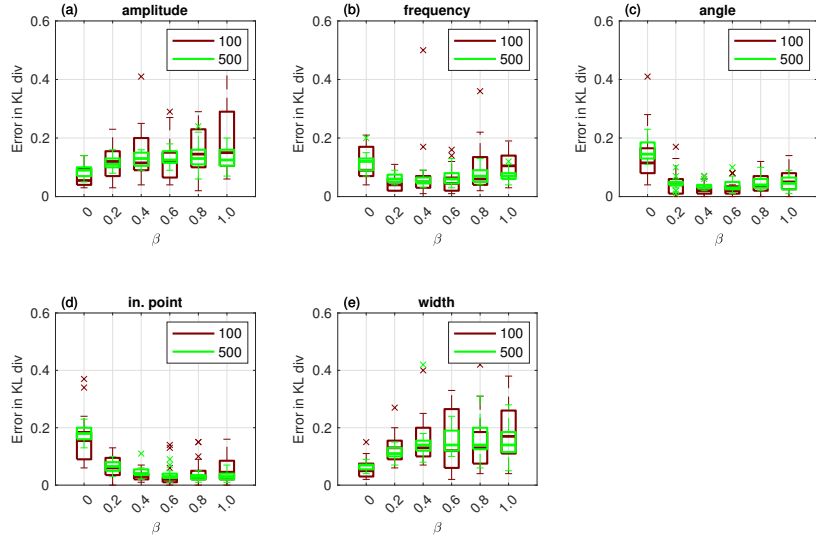


Figure 5. The same as Fig. 4 but using optimal transport resampling.

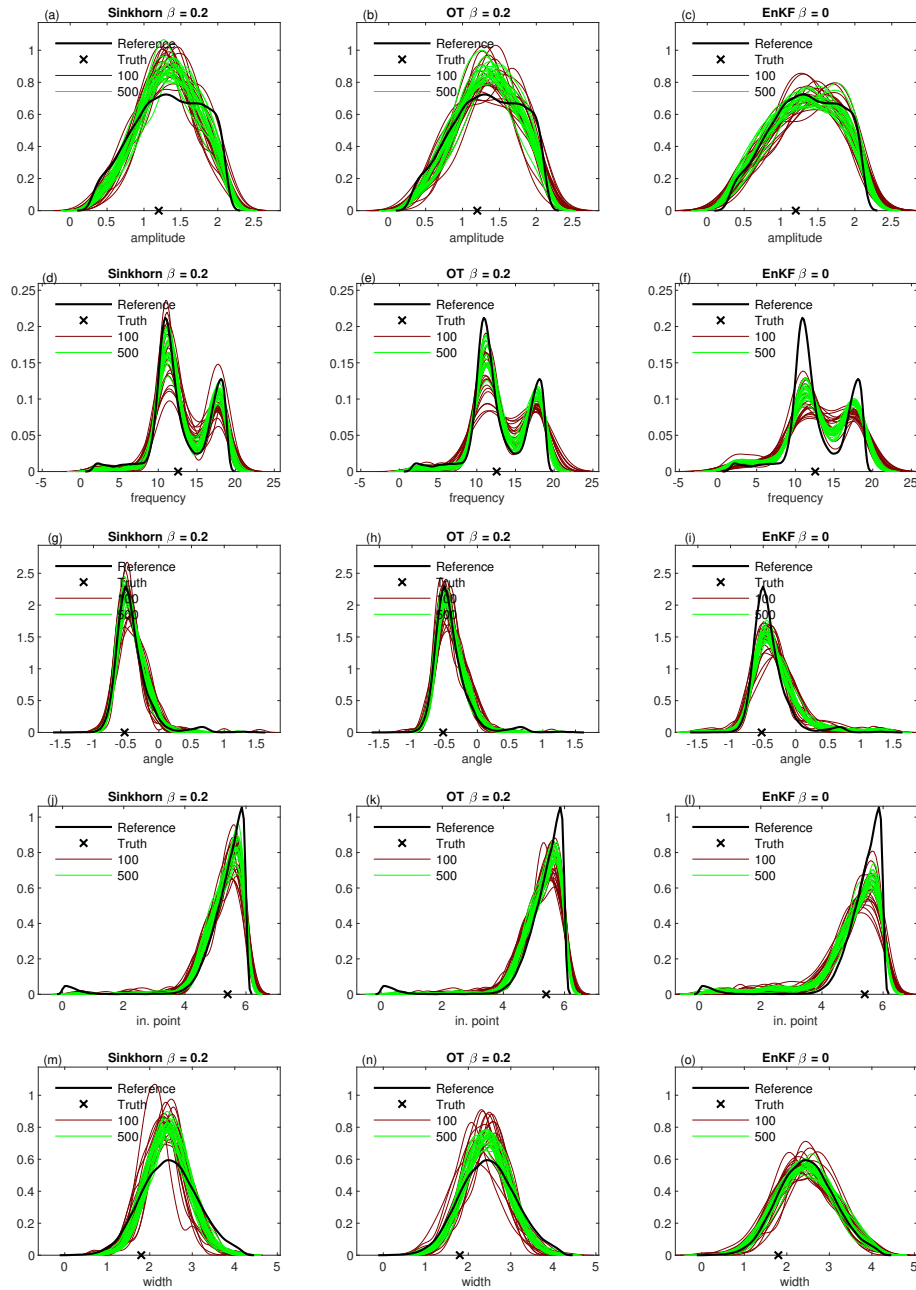


Figure 6. Posterior of geometrical parameters for F2 inference: amplitude (a)–(c), frequency (d)–(f), angle (g)–(i), initial point (j)–(l), and width (m)–(o). On the left is TESPf(0.2); in the middle is TETPF(0.2), and on the right is EnKF. In black is reference, in red 20 simulations of ensemble size $M = 100$, in green 20 simulations of ensemble size $M = 500$. The true parameters are shown as black cross.

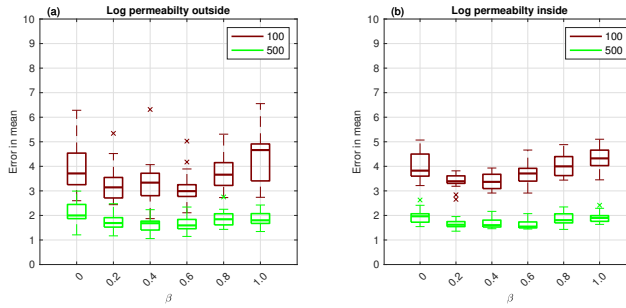


Figure 7. Application to F2 parameterization with Sinkhorn approximation. Box plot over 20 independent simulations of RMSE of mean log permeability outside channel (a) and inside channel (b). X-axis is for the hybrid parameter, where $\beta = 0$ corresponds to EnKF and $\beta = 1$ to TET(S)PF. Ensemble size $M = 100$ is shown in red, and $M = 500$ in green. Central mark is the median, edges of the box are the 25th and 75th percentiles, whiskers extend to the most extreme data points, and crosses are outliers.

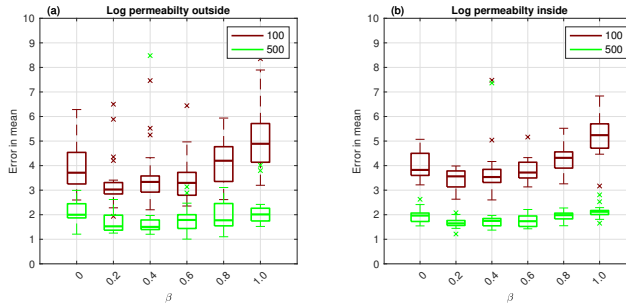


Figure 8. The same as Fig. 7 but using optimal transport resampling.

the channelized domain at ensemble size $M = 100$ and a smallest RMSE over 20 simulations in Fig. 9(b)–(f) and of reference in Fig. 9(a). We see that TESPf(0.2) does an excellent job at such a small ensemble size by estimating well log permeability outside and inside channel, and parameters of the channel itself.

390 4 Conclusions

A Sinkhorn adaptation, namely the TESPf, of the previously proposed TETPF has been introduced and numerically investigated on a parameter estimation problem. The TESPf has similar accuracy results than the TETPF (see Fig. 7, 8 and 6) while it can have considerable smaller computational complexity. Specifically, the TESPf has compexity $\mathcal{O}[T(MC + M^2C(\alpha) + \tau_{\max}MC)]$ and the TETPF $\mathcal{O}[T(MC + M^3 \log M + \tau_{\max}MC)]$, (for a complete overview see table B1). In particular, the TESPf
395 outperforms the EnKF for non-Gaussian distributed parameters (e.g., initial point and angle in F2). This makes the proposed method a promising option for the high-dimensional nonlinear problems one is typically faced with in reservoir engineering. Further, to counter balance potential robustness problems of the TETPF and its Sinkhorn adaptation a hybrid between EnKF and TET(S)PF is proposed and studied by means of the two configurations of the steady-state single-phase Darcy flow model.

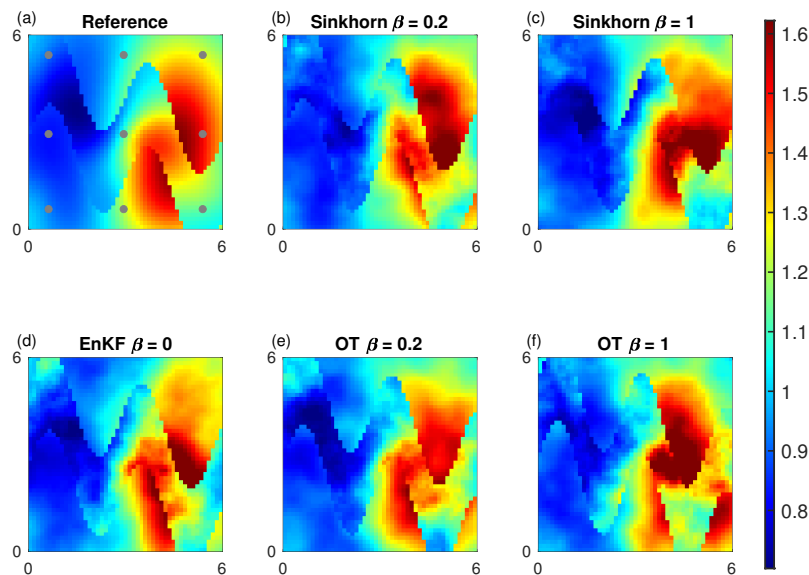


Figure 9. Mean log permeability for F2 inference for the lowest error at ensemble size $M = 100$. Observation locations are shown in circles. Reference (a), TESPF(0.2) (b), TESPF (c), EnKF (d), TETPF(0.2) (e), and TETPF (f).

The combination of the two adaptive SMC methods with complementing properties, i.e., $\beta \in (0, 1)$, is superior to the individual
 400 adaptive SMC method, i.e., $\beta = 0$ or 1 , for all non-Gaussian distributed parameters and performs better than the pure TETPF
 and the TETSPF for Gaussian distributed parameters in F1. This suggests a hybrid approach has a great potential to obtain
 robust and highly-accurate approximate solutions of nonlinear high-dimensional Bayesian inference problems. Note that we
 have considered a synthetic case, where the truth is available, and thus chose β in terms of accuracy of an estimate. However,
 in a realistic application the truth is not provided. In the context of state estimation with an underlying dynamical system it has
 405 been suggested to adaptively change the hybrid parameter with respect to the effective sample size. As the tempering scheme is
 already changed according to the effective sample size this ansatz would require to define the interplay between the two tuning
 variables. An ad-hoc choice for β could be 0.2 or 0.3. This is motivated by the fact that the particle filter is too unstable in high
 dimensions and it is therefore sensible to use a tuning parameter prioritising the EnKF. The ad-hoc choice is supported by the
 numerical results in Section 3 and in Acevedo et al. (2017); de Wiljes et al. (2020) in the context of state-estimation.

Algorithm 1 Sample mutation

Require: $\theta \in (0, 1)$ and an integer τ_{\max} **for** $i = 1, \dots, M$ **do**Initialize $\mathbf{v}_i(0) = \tilde{\mathbf{u}}_{t,i}$ **while** $\tau \leq \tau_{\max}$ **do**Propose $\mathbf{v}_i^{\text{prop}}$ using Eq. (5) for Gaussian probability or Eq. (6) for uniform probabilitySet $\mathbf{v}_i(\tau + 1) = \mathbf{v}_i^{\text{prop}}$ with probability Eq. (7) and set $\mathbf{v}_i(\tau + 1) = \tilde{\mathbf{u}}_{t,i}$ with probability Eq. (8) $\tau \leftarrow \tau + 1$ **end while**Set $\mathbf{u}_{t,i} = \mathbf{v}_i(\tau_{\max})$ **end for**

Algorithm 2 Resampling based on optimal transport

Require: $\{\mathbf{u}_{t-1,i}\}_{i=1}^M$ and $\mathbf{w}_{t-1} = \{w_{t-1,1}, \dots, w_{t-1,M}\}$ Compute \mathbf{Z} with $z_{ij} = \|\mathbf{u}_{t-1,i} - \mathbf{u}_{t-1,j}\|^2$ Supply \mathbf{Z} and \mathbf{w}_{t-1} to the FastEMD algorithm of Pele & Werman with the output being the coupling \mathbf{S} Compute new samples $\{\tilde{\mathbf{u}}_{t,i}\}_{i=1}^M$ from Eq. (11)

Algorithm 3 Sinkhorn iteration for optimal transport problem with entropic regularisation

Require: regularisation parameter α , $\{\mathbf{u}_{t-1,i}\}_{i=1}^M$ and $\mathbf{w}_{t-1} = \{w_{t-1,1}, \dots, w_{t-1,M}\}$ Compute \mathbf{Z} with $z_{ij} = \|\mathbf{u}_{t-1,i} - \mathbf{u}_{t-1,j}\|^2$ Normalise \mathbf{Z} with respect to its maximum entry**while** $\varepsilon \geq 1.0e - 8$ **do** $\mathbf{b} = \mathbf{w}_{t-1} \cdot [\exp(-\alpha \mathbf{Z}) \mathbf{a}]$ $\mathbf{a} = \left(\frac{1}{M} \mathbf{I}_M / M \right) \cdot [\exp(-\alpha \mathbf{Z}) \mathbf{b}]$ $\mathbf{S} = \text{diag}(\mathbf{b}) \exp(-\alpha \mathbf{Z}) \text{diag}(\mathbf{a})$ $\hat{\mathbf{w}} = \mathbf{S} \mathbf{I}_M$ $\varepsilon = \|\hat{\mathbf{w}} - \mathbf{w}_{t-1}\|$ **end while****return** $\mathbf{S}^* = \mathbf{S}$

Appendix B: Computational Complexity

Algorithm 4 Adaptive SMC: TET(S)PF

Require: an initial ensemble $\{\mathbf{u}_{0,i}\}_{i=1}^M \sim \mu_0$, $\theta \in (0, 1)$ and integers τ_{\max} and $1 < M_{\text{thresh}} < M$

Set $\phi_0 = 0$

while $\phi_t \leq 1$ **do**

$t \rightarrow t + 1$

 Compute the likelihood $g(\mathbf{u}_{t-1,i}; \mathbf{y}_{\text{obs}})$ from Eq. (2) (for $i = 1, \dots, M$)

 Compute the tempering parameter ϕ_t :

if $\min_{\phi \in (\phi_{t-1}, 1)} \text{ESS}_t(\phi) > M_{\text{thresh}}$ **then**

 set $\phi_t = 1$

else

 compute ϕ_t such that $\text{ESS}_t(\phi) \approx M_{\text{thresh}}$ using a bisection algorithm on $(\phi_{t-1}, 1]$

end if

 Compute weights $\mathbf{w}_{t-1} = \{w_{t-1,1}, \dots, w_{t-1,M}\}$ from Eq. (3)

 Create new samples $\{\tilde{\mathbf{u}}_{t,i}\}_{i=1}^M$ using optimal (Sinkhorn) resampling via Algorithm 2(3)

 Compute $\{\mathbf{u}_{t,i}\}_{i=1}^M$ using sample mutation via Algorithm 1

end while

Algorithm 5 EnKF

Require: an initial ensemble $\{\mathbf{u}_{0,i}\}_{i=1}^M \sim \mu_0$, $\theta \in (0, 1)$ and integers τ_{\max} and $1 < M_{\text{thresh}} < M$

Set $\phi_0 = 0$

while $\phi_t \leq 1$ **do**

$t \rightarrow t + 1$

 Compute the likelihood $g(\mathbf{u}_{t-1,i}; \mathbf{y}_{\text{obs}})$ from Eq. (2) (for $i = 1, \dots, M$)

 Compute the tempering parameter ϕ_t :

if $\min_{\phi \in (\phi_{t-1}, 1)} \text{ESS}_t(\phi) > M_{\text{thresh}}$ **then**

 set $\phi_t = 1$

else

 compute ϕ_t such that $\text{ESS}_t(\phi) \approx M_{\text{thresh}}$ using a bisection algorithm on $(\phi_{t-1}, 1]$

end if

 Create new samples $\{\tilde{\mathbf{u}}_{t,i}\}_{i=1}^M$ using Eq. (13)

 Compute $\{\mathbf{u}_{t,i}\}_{i=1}^M$ using sample mutation via Algorithm 1

end while

Algorithm 6 Hybrid EnKF-TET(S)PF

Require: initial ensemble $\{\mathbf{u}_{0,i}\}_{i=1}^M \sim \mu_0$, $\theta \in (0, 1)$, hybrid parameter β and integers τ_{\max} and $1 < M_{\text{thresh}} < M$

Set $\phi_0 = 0$

while $\phi_t \leq 1$ **do**

$t \rightarrow t + 1$

Compute the likelihood $g_1(\mathbf{u}_{t-1,i}; \mathbf{y}_{\text{obs}})$ from Eq. (14) (for $i = 1, \dots, M$)

Set $g(\mathbf{u}_{t-1,i}; \mathbf{y}_{\text{obs}}) = g_1(\mathbf{u}_{t-1,i}; \mathbf{y}_{\text{obs}})$ (for $i = 1, \dots, M$)

Compute the tempering parameter ϕ_t :

if $\min_{\phi \in (\phi_{t-1}, 1)} \text{ESS}_t(\phi) > M_{\text{thresh}}$ **then**

set $\phi_t = 1$

else

compute ϕ_t such that $\text{ESS}_t(\phi) \approx M_{\text{thresh}}$ using a bisection algorithm on $(\phi_{t-1}, 1]$

end if

Create new samples $\{\tilde{\mathbf{u}}_{t,i}^\beta\}_{i=1}^M$ using Eq. (13)

Compute the likelihood $g_2(\tilde{\mathbf{u}}_{t,i}^\beta; \mathbf{y}_{\text{obs}})$ from Eq. (15) (for $i = 1, \dots, M$)

Set $g(\mathbf{u}_{t-1,i}; \mathbf{y}_{\text{obs}}) = g_2(\tilde{\mathbf{u}}_{t,i}^\beta; \mathbf{y}_{\text{obs}})$ (for $i = 1, \dots, M$)

Compute weights $\mathbf{w}_{t-1} = \{w_{t-1,1}, \dots, w_{t-1,M}\}$ from Eq. (3)

Create new samples $\{\tilde{\mathbf{u}}_{t,i}\}_{i=1}^M$ using optimal (Sinkhorn) resampling via Algorithm 2(3)

Compute $\{\mathbf{u}_{t,i}\}_{i=1}^M$ using sample mutation via Algorithm 1

end while

Algorithm	Complexity
TETPF	$\mathcal{O}[T(MC + M^3 \log M + \tau_{\max} MC)]$
TESPF	$\mathcal{O}[T(MC + M^2 C(\alpha) + \tau_{\max} MC)]$
EnKF	$\mathcal{O}[T(MC + \kappa^2 n + \tau_{\max} MC)]$
Hybrid EnKF-TETPF	$\mathcal{O}[T(MC + \kappa^2 n + MC + M^3 \log M + \tau_{\max} MC)]$
Hybrid EnKF-TESPF	$\mathcal{O}[T(MC + \kappa^2 n + MC + M^2 C(\alpha) + \tau_{\max} MC)]$
Forward model G	$\mathcal{O}(MC)$
pcn-MCMC mutation	$\mathcal{O}(\tau_{\max} MC)$
FastEMD	$\mathcal{O}(M^3 \log M)$
Sinkhorn approximation	$\mathcal{O}(M^2 C(\alpha))$

Table B1. The table provides an overview of the computational complexity of all the algorithms considered in the manuscript.

Data availability. Data and MATLAB codes for generating the plots are available in Ruchi et al. (2020).

Author contributions. S.R., S.D. and J.dW. designed the research, S.D. ran the numerical experiments, S.R., S.D. and J.dW. analyzed the results and wrote the manuscript.

415 *Competing interests.* The authors declare that they have no conflict of interest.

Acknowledgements. The research of J.dW. and S.R. have been partially funded by Deutsche Forschungsgemeinschaft (DFG) - SFB1294/1 - 318763901. Further J.dW. has been supported by Simons CRM Scholar-in-Residence Program and ERC Advanced Grant ACRCC (grant 339390). S.R. has been supported by the research programme Shell-NWO/FOM Computational Sciences for Energy Research (CSER) with project number 14CSER007 which is partly financed by the Netherlands Organization for Scientific Research (NWO).

420 References

- Acevedo, W., de Wiljes, J., and Reich, S.: Second-order Accurate Ensemble Transform Particle Filters, *SIAM J. Sci. Comput.*, 39, A1834–A1850, 2017.
- Agapiou, S., Papaspiliopoulos, O., Sanz-Alonso, D., and Stuart, A. M.: Importance sampling: computational complexity and intrinsic dimension, *Statistical Science*, 32, 405–431, <https://doi.org/10.1214/17-STS611>, 2017.
- 425 Anderson, J.: An ensemble adjustment Kalman filter for data assimilation, *Monthly Weather Review*, 129, 2884–2903, 2001.
- Bardsley, J., Solonen, A., Haario, H., and Laine, M.: Randomize-then-optimize: A method for sampling from posterior distributions in nonlinear inverse problems, *SIAM J. Sci. Comput.*, 36, A1895–A1910, 2014.
- Beskos, A., Crisan, D., and Jasra, A.: On the stability of sequential Monte Carlo methods in high dimensions, *Ann. Appl. Probab.*, 24, 1396–1445, <https://doi.org/10.1214/13-AAP951>, 2014.
- 430 Beskos, A., Jasra, A., Muzaffer, E. A., and Stuart, A. M.: Sequential Monte Carlo methods for Bayesian elliptic inverse problems, *Statistics and Computing*, 25, 727–737, <https://doi.org/10.1007/s11222-015-9556-7>, 2015.
- Blömker, D., Schillings, C., Wacker, P., and Weissmann, S.: Well posedness and convergence analysis of the ensemble Kalman inversion, *Inverse Problems*, 35, 085 007, <https://doi.org/10.1088/1361-6420/ab149c>, <https://doi.org/10.1088/1361-6420/2Fab149c>, 2019.
- Burgers, G., Leeuwen, P., and Evensen, G.: Analysis Scheme in the Ensemble Kalman Filter, *Monthly Weather Review*, 126, 1719–1724, [https://doi.org/10.1175/1520-0493\(1998\)126<1719:ASITEK>2.0.CO;2](https://doi.org/10.1175/1520-0493(1998)126<1719:ASITEK>2.0.CO;2), 1998.
- 435 Carrassi, A., Bocquet, M., Bertino, ., and Evensen, G.: Data assimilation in the geosciences: An overview of methods, issues, and perspectives, *WIREs Climate Change*, 9, e535, <https://doi.org/10.1002/wcc.535>, 2018.
- Chada, N., Iglesias, M., Roininen, L., and Stuart, A.: Parameterizations for Ensemble Kalman Inversion, *Inverse Problems*, 34, 055 009, 2018.
- 440 Chen, Y. and Oliver, D.: Ensemble randomized maximum likelihood method as an iterative ensemble smoother, *Math. Geosci.*, 44, 1–26, 2012.
- Chustagulprom, N., Reich, S., and Reinhardt, M.: A Hybrid Ensemble Transform Particle Filter for Nonlinear and Spatially Extended Dynamical Systems, *SIAM/ASA Journal on Uncertainty Quantification*, 4, 592–608, <https://doi.org/10.1137/15M1040967>, 2016.
- Cotter, S., Roberts, G., Stuart, A., and White, D.: MCMC methods for functions: modifying old algorithms to make them faster, *Statistical Science*, 28, 424–446, 2013.
- 445 Cuturi, M.: Sinkhorn Distances: Lightspeed Computation of Optimal Transport, in: *Advances in Neural Information Processing Systems* 26, edited by Burges, C. J. C., Bottou, L., Welling, M., Ghahramani, Z., and Weinberger, K. Q., pp. 2292–2300, Curran Associates, Inc., <http://papers.nips.cc/paper/4927-sinkhorn-distances-lightspeed-computation-of-optimal-transport.pdf>, 2013.
- Dashti, M. and Stuart, A. M.: *The Bayesian Approach to Inverse Problems*, pp. 311–428, Springer International Publishing, Cham, https://doi.org/10.1007/978-3-319-12385-1_7, 2017.
- 450 de Wiljes, J., Pathiraja, S., and Reich, S.: Ensemble Transform Algorithms for Nonlinear Smoothing Problems, *SIAM J. Sci. Comput.*, 42, A87–A114, 2020.
- Del Moral, P., Doucet, A., and Jasra, A.: Sequential Monte Carlo samplers, *Journal of the Royal Statistical Society: Series B (Statistical Methodology)*, 68, 411–436, <https://doi.org/10.1111/j.1467-9868.2006.00553.x>, 2006.
- 455 Emerick, A. and Reynolds, A.: Ensemble smoother with multiple data assimilation, *Computers & Geosciences*, 55, 3–15, 2013.

- Ernst, O. G., Sprungk, B., and Starkloff, H.-J.: Analysis of the Ensemble and Polynomial Chaos Kalman Filters in Bayesian Inverse Problems, *SIAM/ASA Journal on Uncertainty Quantification*, 3, 823–851, <https://doi.org/10.1137/140981319>, 2015.
- Frei, M. and Künsch, H.: Bridging the ensemble Kalman and particle filters, *Biometrika*, 100, 781–800, 2013.
- Frei, M. and Künsch, H. R.: Bridging the ensemble Kalman and particle filters, *Biometrika*, 100, 781–800, <https://doi.org/10.1093/biomet/ast020>, 2013.
- Hairer, M., Stuart, A., and Vollmer, S.: Spectral gaps for a Metropolis–Hastings algorithm in infinite dimensions, *Ann. Appl. Probab.*, 24, 2455–2490, 2014.
- Houtekamer, P. L. and Zhang, F.: Review of the Ensemble Kalman Filter for Atmospheric Data Assimilation, *Monthly Weather Review*, 144, 4489–4532, <https://doi.org/10.1175/MWR-D-15-0440.1>, 2016.
- Iglesias, M., Park, M., and Tretyakov, M.: Bayesian inversion in resin transfer molding, *Inverse Problems*, 34, 105 002, 2018.
- Iglesias, M. A.: A regularizing iterative ensemble Kalman method for PDE-constrained inverse problems, *Inverse Problems*, 32, 025 002, 2016.
- Iglesias, M. A., Lin, K., and Stuart, A. M.: Well-posed Bayesian geometric inverse problems arising in subsurface flow, *inverse problems*, 30, 114 001, 2014.
- Kantorovich, L. V.: On the translocation of masses, in: *Dokl. Akad. Nauk. USSR (NS)*, vol. 37, pp. 199–201, 1942.
- Liu, Y., Haussaire, J., Bocquet, M., Roustan, Y., Saunier, O., and Mathieu, A.: Uncertainty quantification of pollutant source retrieval: comparison of Bayesian methods with application to the Chernobyl and Fukushima-Daiichi accidental releases of radionuclides, *Q. J. R. Meteorol. Soc.*, 143, 2886–2901, 2017.
- Lorentzen, R. J., Bhakta, T., Grana, D., Luo, X., Valestrand, R., and Nævdal, G.: Simultaneous assimilation of production and seismic data: application to the Norne field, *Computational Geosciences*, 24, 907–920, <https://doi.org/10.1007/s10596-019-09900-0>, 2020.
- Matérn, B.: *Spatial Variation*, Lecture Notes in Statistics, No. 36, Springer, 1986.
- Monge, G.: *Mémoire sur la théorie des déblais et des remblais*, *Histoire de l’Académie Royale des Sciences de Paris*, 1781.
- Neal, R. M.: Annealed importance sampling, *Statistics and computing*, 11, 125–139, 2001.
- Oliver, D., He, N., and Reynolds, A.: Conditioning permeability fields to pressure data, *ECMOR V-5th European Conference on the Mathematics of Oil Recovery*, pp. 259–269, 1996.
- Pele, O. and Werman, M.: Fast and robust earth mover’s distances, in: *Computer vision, 2009 IEEE 12th international conference on*, pp. 460–467, IEEE, 2009.
- Peyré, G. and Cuturi, M.: *Computational Optimal Transport: With Applications to Data Science*, 2019.
- Reich, S.: A nonparametric ensemble transform method for Bayesian inference, *SIAM Journal on Scientific Computing*, 35, A2013–A2024, 2013.
- Roberts, G. O. and Rosenthal, J. S.: Optimal scaling for various Metropolis-Hastings algorithms, *Statist. Sci.*, 16, 351–367, <https://doi.org/10.1214/ss/1015346320>, 2001.
- Ruchi, S., Dubinkina, S., and Iglesias, M. A.: Tempered ensemble transform particle filter for non-Gaussian elliptic problems, *Inverse Problems*, 35, 115 005, 2019.
- Ruchi, S., Dubinkina, S., and de Wiljes, J.: Data underlying the paper: Fast hybrid tempered ensemble transform filter formulation for Bayesian elliptical problems via Sinkhorn approximation, *4TU, Centre for Research Data, Dataset*, <https://doi.org/10.4121/12987719>, 2020.

- Santitissadeekorn, N. and Jones, C.: Two-Stage Filtering for Joint State-Parameter Estimation, *Monthly Weather Review*, 143, 2028–2042, <https://doi.org/10.1175/MWR-D-14-00176.1>, 2015.
- 495 Sinkhorn, R.: Diagonal equivalence to matrices with prescribed row and column sums, *The American Mathematical Monthly*, 74, 402–405, 1967.
- Stordal, A., Karlsen, H. A., Nævdal, G., Skaug, H., and Vallès, B.: Bridging the ensemble Kalman filter and particle filters: the adaptive Gaussian mixture filter, *Computational Geosciences*, 15, 293–305, <https://doi.org/10.1007/s10596-010-9207-1>, 2011.
- Stuart, A. M.: Inverse problems: a Bayesian perspective, *Acta Numerica*, 19, 451–559, 2010.
- 500 Vergé, C., Dubarry, C., Del Moral, P., and Moulines, E.: On parallel implementation of sequential Monte Carlo methods: the island particle model, *Statistics and Computing*, 25, 243–260, <https://doi.org/10.1007/s11222-013-9429-x>, 2015.
- Zovi, F., Camporese, M., Hendricks Franssen, H.-J., Huisman, J. A., and Salandin, P.: Identification of high-permeability subsurface structures with multiple point geostatistics and normal score ensemble Kalman filter, *Journal of Hydrology*, 548, 208–224, <https://doi.org/https://doi.org/10.1016/j.jhydrol.2017.02.056>, 2017.